

# Supporting Information

Rauhut et al. 10.1073/pnas.1203238109

## SI Methods: UV Photography

Most fossil skeletal remains and some mineralized soft parts from the Upper Jurassic plattenkalks of southern Germany and from the Middle to Late Mesozoic localities of Northeastern China are fluorescent under UV radiation. In most cases, this fluorescence allows a more precise investigation of morphological details of skeletal remains as well as soft parts. Delicate skeletal elements and remains of soft parts are poorly or not discernable in visible light but shine conspicuously under filtered UV. The technique can be used to differentiate bone sutures from cracks, to establish outlines of compressed skeletal elements more clearly, and to separate bones or soft parts from the underlying matrix and from each other.

During the past 10 y, H.T. has considerably improved techniques of UV investigation and UV-light photography of fossils from Solnhofen and Solnhofen-type Lagerstätten as well as from the Middle Jurassic to Early Cretaceous lacustrine deposits of the Jinlingsi and Jehol Group, Northeastern China, using powerful UV lamps and photographic documentation techniques (1–9). For our investigations we predominantly use UVA lamps with a wavelength of 365–366 nm.

Sometimes essential details of bones and soft parts are poorly or not visible to the naked eye or even under a microscope using UV light and can be demonstrated only by UV-light photography. The use of different filters allows selective visualization of peculiar fine structures. In most cases, a variety of different color-correction filters is necessary. Each limestone slab and bone or tissue reacts differently to different light wavelengths and is captured differently with varying exposures and filters. The right combination is needed to highlight the area of interest. The optimum filtering and exposure time must be tested in a series of experiments (1). The number and combination of filters varies greatly, and exposure times vary between 1 s and several minutes, depending on the nature of the fossil material and the magnification, intensity, and incident angle of the UV lamps. Filtering works optimally with analog photography using slide films, although digital cameras can be used also.

## Additional Information on *Sciurumimus*

**History of Find and Preparation of Specimen.** The specimen was found during systematic excavations in the Rygol Quarry at Painten, Bavaria, Germany. First, the bony elements of the central area of the body appeared after cleaning on the floor of the excavation area, so the slab with the skeleton was excavated and brought into the laboratory for preparation. In the laboratory, the upper surface (the surface exposed in the quarry) was stabilized with ceramic glue (Knauf Uniflott) and was fixed to another slab. Then, the specimen was prepared mechanically from the underside. Damaged areas were reconstructed with Mapei Keraquick, which is clearly visible under UV light. Loose bones and sections were glued onto the specimen, but no arrangement or orientation of bones was changed. The specimen was studied by H.T. before preparation, so there can be no doubt about its authenticity.

## Selected measurements for *Sciurumimus albersdoerferi*:

Total length of skeleton	719 mm
Skull length	79 mm
Posterior skull height	ca. 32 mm

Length of orbit	19.7 mm
Height of orbit	21.5 mm
Length of mandible	73.2 mm
Length of cervical series	69 mm
Length of dorsal series	102 mm
Length of sacrum	37.25 mm
Length of preserved caudal series	432 mm
Length of humerus	26.8 mm
Length of radius	17 mm
Length of metacarpal II	11 mm
Length of femur	50.6 mm
Length of tibiotarsus	54.2 mm
Length of metatarsal III	32.1 mm

**Ontogenetic Stage of the Specimen.** Although no histological sampling is possible in this unique specimen, several lines of evidence indicate that the holotype is an early juvenile, probably an early-posthatchling individual.

First, there is no fusion of any skeletal elements in the skeleton. In the vertebral column, the neurocentral sutures of the cervical, dorsal, and at least anterior caudal vertebrae are open, and the neural arches have disarticulated slightly from the centra in at least some elements. The sacral centra are preserved in articulation, but the posterior two sacrals are displaced ventrally from the anterior end of the sacrum, demonstrating that the sacral vertebrae have not fused with each other, nor have the sacral ribs fused with the ilium. Although the pattern of neurocentral suture closure varies among dinosaurs (10), the lack of fusion in all vertebrae, with the possible exception of the distal-most caudals [which already are closed in hatchling crocodiles (11)], clearly indicates that the specimen of *Sciurumimus* is an immature individual. This identification is supported further by disarticulation in other elements that usually show very tight sutures or even fusion in theropods, such as the basioccipital and exoccipital or the distal ischium. Likewise, several skeletal elements, such as the carpal and distal tarsal bones, show poor ossification, and several joint surfaces, including the proximal articular end of the humerus, exhibit strongly porous surfaces, indicating poorly ossified articular ends.

Another indicator of the early juvenile stage of *Sciurumimus* is found in the surface structure of basically all bony elements. Both dermal and enchondral elements show a coarsely striated surface (Figs. S4 and S5). Such a surface structure corresponds to bone texture type I of Tumarkin-Deratzian et al. (12). According to these authors, in birds this texture occurs only in individuals of 50% or less skeletal maturity (i.e., hatching-year birds). Bone surface textures were found to be a useful ontogenetic indicator in a number of fossil amniotes (summarized in ref. 13), and thus this texture type represents an independent indication of an early ontogenetic stage for the specimen.

Finally, the maxillary dentition of *Sciurumimus* shows a conspicuous pattern of fully erupted teeth intercalated with empty tooth positions. A very similar pattern in *Scipionyx* was interpreted as an indication that no complete wave of tooth replacement had occurred (14), again indicating an early-posthatchling stage for the animal.

If the presence of a frontoparietal gap can be substantiated by future studies, that presence would represent a further ar-

gument for regarding the specimen as an early-posthatchling individual (15).

Given this early ontogenetic stage of the type specimen of *Sciurumimus*, the small size of the specimen does not necessarily indicate that this taxon was a small theropod as an adult. Indeed, a hatchling *Allosaurus* maxilla described in ref. 16 is considerably smaller (23 mm) than the same element in *Sciurumimus* (42 mm), although *Allosaurus* grows to sizes in excess of 7 m. Thus, unless *Sciurumimus* had a strongly reduced growth rate, as is the case in island dwarf sauropods (17, 18), this taxon probably grew to adult sizes in excess of 5 m, as did other megalosaurids.

**Phylogenetic Analysis.** To establish the phylogenetic position of *Sciurumimus*, we coded it into three recent phylogenetic analyses. Two of these analyses, those of Smith et al. (19) and of Choiniere et al. (20), were chosen because they are among the largest theropod analyses published thus far, including a high number of characters and a taxon sampling that represents all major groups of nonavian theropods. Both these analyses consistently depicted *Sciurumimus* as a basal tetanuran, although with rather poor resolution at the base of this clade and somewhat differing results (see below). Therefore, we ran a third analysis, using the most comprehensive matrix on basal tetanurans published so far, that of Benson et al. (21). The results of the third analysis were used for the phylogenetic placement of *Sciurumimus* presented in this paper.

Given the juvenile status of the specimen, one important question, of course, is the possible effect of ontogenetically variable characters on its phylogenetic position. Clearly age-dependent characters, such as fusion of skeletal elements, were coded as “?” for *Sciurumimus* in all analyses. Furthermore, in addition to the analyses reported below, we ran additional analyses of the three data matrices with all characters we considered potentially variable with ontogeny [e.g., characters concerning cranial ornamentation (crests, rugosities), orbit shape and size, morphometric ratios between different elements or between different structures within one element, development of muscle attachments] coded as “?” for *Sciurumimus*. Although this characterization considerably increased the amount of missing data in *Sciurumimus*, the phylogenetic results remained the same as those reported below.

**Analysis based on Smith et al.** Smith et al. (19) presented a phylogenetic analysis of six outgroup and 51 neotheropod ingroup taxa, plus one single specimen from the Early Cretaceous of Australia, coded across 353 morphological characters. This matrix is a slightly expanded version of the matrix of Smith et al. in ref. 22 and includes a wide array of nonavian theropods, from coelophysoids to paravians, although with emphasis on non-coelurosaurian forms [39 of the ingroup operational taxonomic units (OTUs)]. We coded *Sciurumimus* in the same matrix, without changes to other codings, and ran the analysis in PAUP\* 4.0 (<http://paup.csit.fsu.edu/>), using a heuristic search with tree bisection and reconnection (TBR) branch swapping and random addition sequence with 100 replicates. The analysis resulted in the recovery of 3,720 equally parsimonious trees with a length of 887 steps. The strict consensus of these trees (Fig. S6) generally agrees with that found by Smith et al. (19), although with slightly less resolution within Megalosauroidea (= Spinosauroidae). *Sciurumimus* was found to be the sister taxon to *Monolophosaurus* and Neotetanurae in this analysis. However, only one additional step is needed to place this taxon within Megalosauroidea, whereas a placement within Neotetanurae requires at least six additional steps. Tree support is low, with bootstrap values below 50 for the vast majority of nodes within Theropoda, with the exception of some coelurosaur clades.

Codings for *Sciurumimus* in the matrix of Smith et al. (19) are as follows:

```
00200[0/1]0101??100?10?000?21000011???00?00?10-1[1/2]0?
01????0001000?00???00?000?????0121??0?0?100????
00000?????????????????0100100?11?1000[0/1]0?11?0110?
1110[0/1]?0?0?0120?00?00101????000?10020????000??
0010001000000?????01[0/1]000000[0/1]000000?00?
011111010110?010010000000?001100?1?[0/1]1?0?0???00?
10?00000011?0?1??201?????10?????????00????????????
1100?0?01??1201?0000100
```

**Analysis based on Choiniere et al.** In the supplementary information of their paper, Choiniere et al. (20) presented one of the largest phylogenetic analyses of nonavian theropods published so far, including two outgroup and 92 neotheropodan ingroup taxa, scored across 421 characters. Like the analysis of Smith et al. (19), this analysis includes a wide array of taxa, but with an emphasis on coelurosaur (71 of the ingroup taxa). *Sciurumimus* was coded for the 421 characters of Choiniere et al. (20), and the analysis was run in TNT 1.1 (23), using a heuristic search strategy with random addition sequence, performing 1,000 replicates of Wagner trees, followed by TBR branch swapping. TNT was chosen as analytic program for this matrix because analysis in PAUP was prohibitively long. The analysis resulted in 1,210 equally parsimonious trees with a length of 1,866 steps. The strict consensus tree agrees with that found by Choiniere et al. (20), and *Sciurumimus* was found to be a basal, nonneotetanuran tetanuran, forming a polytomy with *Afrovenator* and a spinosaurid-*Torvosaurus* clade (Fig. S7).

Codings for *Sciurumimus* in the matrix of Choiniere et al. (20) are as follows:

```
10?0[01]00?00?11010?????20001?00?0?0000?000?
11100000?21?0010?????000?00???0100???0?10???????
000?????????????000?1?0000?????????0?1000100?01110?
0?011?000?01001?00002000?0?00?0202??[01]0?00111?0?
00?00?00011001?23????0000000000?0000100001000??
1??0000?11000?00001000?0000?000001?1??011100010?
012112111?1000000100?02?0?0?0?0?1?1?0?00?01?0?0?
00001000010?1?000?01??0?000100?????1??1?????
00?????????????0010?00?0?02000?
```

**Analysis based on Benson et al.** After establishing that *Sciurumimus* is a basal, noncoelurosaurian theropod in the analyses of Smith et al. (19) and Choiniere et al. (20), we decided to test its detailed phylogenetic position in the most extensive phylogenetic analysis of basal tetanurans published so far, that of Benson et al. (21). This matrix included four outgroup and 41 tetanuran ingroup taxa, with emphasis on basal, noncoelurosaurian taxa [38 of the ingroup taxa, as opposed to 20 in Smith et al. (19) and 13 in Choiniere et al. (20)], scored across 233 characters. We included *Sciurumimus* in this matrix and reran the analysis in PAUP\* 4.0, using the settings described above for the Smith et al. (19) analysis. The analysis resulted in 7,383 equally parsimonious trees with a length of 656 steps. The strict consensus of these trees placed *Sciurumimus* in a large polytomy within Megalosauroidea more derived than *Monolophosaurus*. After the exclusion of *Piveteausaurus*, a reduced consensus tree depicts *Sciurumimus* as the most basal representative of the Megalosauridae (Fig. 4 and Fig. S8). As in the previous analyses, tree support is rather low, with most clades showing bootstrap values below 50%.

An interesting result of the analysis is that the inclusion of *Sciurumimus*, without any other changes to the original matrix of Benson et al. (21), led to the recovery of the monophyletic Carnosauria, including the Megalosauroidea and Allosauroidae. This relationship also was found by Rauhut (24) but is at variance with most recent analyses, which recovered megalosauroids (or spinosauroids) as an outgroup to a monophyletic Neotetanurae that includes allosauroids and coelurosaur (e.g., refs. 19–21). Synapomorphies of carnosaurs include the presence of

a subnarial foramen, the presence of at least weakly developed enamel wrinkles in the lateral teeth, opisthocoelous cervical vertebrae, a kinked anterior edge of the anterior caudal neural spines, the presence of an indentation between the acromion process of the scapula and the coracoid, a biceps tubercle that is developed as an obliquely oriented ridge, the presence of a broad ridge above the acetabulum on the ilium, and the presence of a well-developed extensor groove on the anterior side of the distal femur. However, making Neotetanurae monophyletic, excluding megalosauroids, requires only two additional steps. Thus, the interrelationships of basal tetanurans remain problematic and need additional investigation.

Codings for *Sciurumimus* in the matrix of Benson et al. (21) are as follows:

```
[0/1]??01?0?1001101?0?????0?0000-010210??010000??
000?0?00??11????00101??1????1?0?110000010020?00101?
00?111?0[1/2]?10[0/1]?11??0000000??001001?00200000?
1????0000[0/1]001011?-0001????[0/1]0?00?0?101001?1??
11??????01??????02??0010?010??00?00?0??
```

## SI Discussion

The congruent results of the three phylogenetic analyses provide strong support for a basal tetanuran relationship of *Sciurumimus*, although some uncertainty about the exact phylogenetic position remains. As demonstrated by the analysis based on the matrix of Benson et al. (21), the combination of characters shown by *Sciurumimus* is most compatible with megalosauroid relationships. Although this outcome is supported by analyses in which all characters that we considered potentially ontogenetically variable were coded as “?” for *Sciurumimus*, the very early ontogenetic stage of the specimen leaves room for speculation about the possible effects of ontogenetic changes on the phylogenetic results, because little is known as yet about ontogenetic changes in nonavian theropod dinosaurs. On the other hand, the results show that even such very young individuals preserve enough phylogenetically relevant information to establish at least their approximate phylogenetic position.

**Comparison with *Juravenator starki*.** At first glance, the skeleton of *Sciurumimus* seems to be strikingly similar to that of *Juravenator starki* from the Kimmeridgian of Schamhaupten (25, 26). The two animals are contemporaneous up to the same horizon within the same ammonite subzone (27), come from the same geographical area (although from different subbasins within the Upper Jurassic limestone deposits of southern Germany), and are of closely matching size. Indeed, even in detailed comparison, the proportions of *Juravenator* and *Sciurumimus* are strikingly similar (Table S1).

However, despite these similarities in general morphometrics, the two taxa show numerous differences in anatomical details (based on ref. 26 and on observations on the type of *Juravenator* by O.W.M.R. and C.F.), even though comparison sometimes is hampered by the different preservation (*Sciurumimus* is exposed in lateral view, but *Juravenator* is exposed in dorsolateral view for most elements; see ref. 26). Thus, in the skull of *Juravenator*, the anterior margin of the antorbital fossa is rectangular, rather than gently rounded, the maxillary fenestra is relatively smaller, the antorbital fossa is smaller, the ventral process of the postorbital is more massive and notably curved, the ventral (quadratojugal) process of the squamosal tapers to a point, and the posterior premaxillary teeth bear serrations, whereas they are more slender and devoid of serrations in *Sciurumimus*. In the vertebral column, *Juravenator* differs from *Sciurumimus* in the following characteristics (in the following all characters listed refer to the situation in *Juravenator*): cervical epiphyses are small, barely (if at all) overhanging the postzygapophyses; prezygoepiphysal laminae

in the cervical vertebrae are absent; a posterior pleurocoel is present in a midcervical centrum; anterior-most dorsal vertebrae are distinctly elongate; neural spines in the anterior caudal vertebrae are triangular and strongly posteriorly inclined; the posterior caudal vertebrae are relatively more elongate; posterior caudal prezygapophyses are more elongate and are directed anteriorly rather than anterodorsally; distal chevrons are skid-like. In the pectoral girdle and forelimb, the following differences can be established: The scapula is less slender and has a distinctly curved blade; the supraglenoid fossa is triangular, with an acutely angled posterior rim; the internal tuberosity of the humerus is confluent with the proximal humeral articular surface, forming a rectangular edge on the medial side of the proximal humerus; the ulna lacks a proximal expansion and olecranon process; and the shaft of the ulna is more massive than the shaft of radius. In the pelvis and hindlimb, *Juravenator* differs from *Sciurumimus* in the lack of an anterior dorsal lip of the ilium (the presence of which represents an autapomorphy of *Sciurumimus*); the relatively smaller pubic peduncle of the ilium; a more reduced supraacetabular crest, which is confluent posteriorly with the lateral brevis shelf; a pronounced antitrochanteric lip on the ischial peduncle of the ilium; a rectangular rather than undulate posterior end of the postacetabular blade of the ilium; an obturator process on the ischium [erroneously identified as pubis by Chiappe and Göhlich (26)] that is offset from the pubic peduncle; the lack of a distal expansion of the ischial shaft; the short and triangular metatarsal I; a metatarsal IV that is distinctly longer than metatarsal II; and the shorter and more robust metatarsal V. These numerous differences strongly indicate that the two animals cannot be referred to the same taxon, despite their similar size and proportions.

Looking at the phylogenetic position of *Juravenator* led to some interesting results. To test the position of this taxon, we also coded it in the matrices of Smith et al. (19) and Choiniere et al. (20) and analyzed the matrices under the parameters outlined above. When analyzed together with *Sciurumimus*, *Juravenator* was found to be the sister taxon to this genus in both analyses, with otherwise no changes in the phylogenetic position of *Sciurumimus* (i.e., both taxa were found to be basal, non-neotetanuran tetanurans). However, when *Sciurumimus* was removed from the analyses, *Juravenator* was found to be a basal coelurosaur in both cases (Figs. S9 and S10).

As is the case with *Sciurumimus*, the type of *Juravenator* most probably is an early-posthatchling individual, because it lacks any fusion of skeletal elements, lacks ossified carpal and distal tarsal elements altogether, and shows a coarsely striated surface texture in all skeletal elements (see ref. 26). Several of the characters shared by *Sciurumimus* and *Juravenator* and interpreted as synapomorphies of these taxa in the analyses probably are ontogenetically variable, e.g., the round orbit, anterodorsally sloping ventral strut of the lacrimal (related to the size and shape of the orbit), absence of a posteroventral process in the coracoid, absence of a ventral hook on the preacetabular blade of the ilium, and poorly developed attachment of the iliofibularis muscle on the fibula (in all three muscle-attachment areas). Thus, analysis of these two early juveniles together with otherwise subadult and adult theropods might give erroneous results, and we consider the phylogenetic position of *Juravenator* to be uncertain. *Juravenator* shows a highly unusual combination of characters (26), and further analysis of its affinities is necessary to establish its phylogenetic position firmly. However, such a detailed reappraisal of *Juravenator* is beyond the scope of this paper.

These phylogenetic results further suggest that the frequent referral of early juvenile theropods such as *Juravenator* (25) and *Scipionyx* (15) to the Compsognathidae simply might reflect the similarities between these taxa and the (also juvenile) type specimen of *Compsognathus longipes*, and thus the phylogenetic status and content of the Compsognathidae should be reevaluated.



*Sciurumimus* specimen helps bridge the considerable gap between both filamentous integument structures. Thus, protofeathers probably represent the plesiomorphic state for dinosaurs (46, 47). However, scaly skin impressions are known in many dinosaur groups (e.g., Ceratopsia, Stegosauria, Hadrosauridae, Sauropodomorpha, Ceratosauria, basal Tetanurae, and basal coelurosaurians) (25, 41, 48–53). These scales usually are nonoverlapping and polygonal in shape (41).

However, we do not regard the presence of both scales and protofeathers in early dinosaurs as problematic. Most fossil skin impressions are incomplete and are preserved only as small, regionally distributed patches; from these impressions one can conclude only that a particular body region was covered with scaly skin. The examples of *Psittacosaurus* and *Juravenator* in which both scales and protofeathers are present show that different integument structures can be present in the same animal. Furthermore, recent studies in evolutionary developmental biology indicate that scale and feather development are regulated by the same set of signal molecules. Thus, only small changes within the pathways can lead to different integument structures (54–57), and it seems likely that feathers could be lost secondarily in several lines independently. Finally, although scaly skin impressions might be preserved in various sediments, including even coarse sandstones, the preservation of fine filaments, such as those found in *Sciurumimus*, requires very special conditions, so taphonomic processes also play a major role in our understanding of the distribution of integumentary structures in theropod dinosaurs. This last conclusion is supported by the recent find of the large tyrannosauroid theropod *Yutyrannus*, which was preserved in a suitable environment and has filamentous feathers preserved (58).

Interestingly, the bodies of pterosaurs also were covered with monofilaments (59, 60), recently named “pynofibers” (7). If filamentous protofeathers are primitive for dinosaurs, it seems very likely that these pynofibers are homologous to the protofeathers of dinosaurs (61), and thus the origin of feathers leads back to ornithodiran origins.

The preserved integument structures of *Sciurumimus* provide additional information on the morphology of protofeathers and

the origin of feathers. In one area, on the dorsal side of the tail, protofeathers and skin are preserved in direct association. The structures can be differentiated by their different luminescence under UV light. The protofeathers seem to be anchored in the skin, indicating that these integument structures might have grown from follicles. Indeed, conspicuous, dorsoventrally elongated skin structures are preserved where the filaments reach the skin; these structures might represent direct evidence for these follicles. This possibility is interesting, because it has been suggested that follicle formation was a late event in feather evolution and took place with the evolution of vaned feathers (62–64). This scenario was based on the feather embryogenesis of some recent bird species, in which barb ridge formation occurs before follicle formation. The hypothesis that unbranched protofeathers apparently grow from a follicle supports the idea that feather evolution is highly correlated with follicle formation (65, 66). Further support for this idea comes from *Psittacosaurus*, in which the bristles extend under the skin layer (44), lending additional support for the homology of ornithischian filaments with theropod protofeathers and bird feathers.

**Repository of the Specimen.** The holotype specimen of *Sciurumimus* belongs to the private Paiten collection of the Albersdörfer family, where it bears the collection number 1687. However, the scientific availability of the specimen is guaranteed by its inclusion in the register of cultural objects of national importance of Germany (Verzeichnis national wertvollen Kulturgutes). Under the Act to Prevent the Exodus of German Cultural Property (KultSchG; Bundesgesetzblatt I: 1754; 1999), the inclusion of the specimen in this list prevents its being sold outside Germany and guarantees that its repository is always known and that changes of repository must be announced. Furthermore, the type specimen of *Sciurumimus albersdoerferi* is deposited as a permanent loan at the municipal Bürgermeister Müller Museum in Solnhofen, Bavaria, where it also is available for additional scientific study and bears the specimen number BMMS BK 11.

- Tischlinger H (2002) The Eichstätt specimen of *Archaeopteryx* under long-wave UV light. *Archaeopteryx* 20:21–38. German.
- Tischlinger H, Unwin DM (2004) UV investigations of the Berlin specimen of *Archaeopteryx lithographica* H. v. Meyer 1861 and the isolated *Archaeopteryx* feather. *Archaeopteryx* 22:17–50. German.
- Tischlinger H (2005) New information on the Berlin specimen of *Archaeopteryx lithographica* H. v. Meyer 1861. *Archaeopteryx* 23:33–50. German.
- Tischlinger H (2005) Ultraviolet light investigations of fossils from the Upper Jurassic plattenkalks of Southern Franconia. *Zitteliana B* 26:26.
- Arratia G, Tischlinger H (2010) The first record of Late Jurassic crossognathiform fishes from Europe and their phylogenetic importance for teleostean phylogeny. *Foss Rec* 13:317–341.
- Hone DWE, Tischlinger H, Xu X, Zhang F (2010) The extent of the preserved feathers on the four-winged dinosaur *Microraptor gui* under ultraviolet light. *PLoS ONE* 5:e9223.
- Kellner AWA, et al. (2010) The soft tissue of *Jeholopterus* (Pterosauria, Anurognathidae, Batrachognathinae) and the structure of the pterosaur wing membrane. *Proc Biol Sci* 277:321–329.
- Schweigert G, Tischlinger H, Dietl G (2010) Eine fossile Feder aus dem Nusplinger Plattenkalk (Oberjura, Schwäbische Alb). *Archaeopteryx* 28:31–40.
- Tischlinger H, Frey E (2010) Multilayered is not enough! New soft tissue structures in the *Rhamphorhynchus* flight membrane. *Acta Geoscientia Sinica* 31:64.
- Irmis RB (2007) Axial skeleton ontogeny in the Parasuchia (Archosauria: Pseudosuchia) and its implications for ontogenetic determination in archosaurs. *J Vert Paleont* 27:350–361.
- Brochu CA (1996) Closure of neurocentral sutures during crocodylian ontogeny: Implications for maturity assessment in fossil archosaurs. *J Vert Paleont* 16:49–62.
- Tumarkin-Deratzian AR, Vann DR, Dodson P (2006) Bone surface texture as an ontogenetic indicator in long bones of the Canada goose *Branta canadensis* (Anseriformes: Anatidae). *Zool J Linn Soc-Lond* 148:133–168.
- Tumarkin-Deratzian AR (2009) Evaluation of long bone surface textures as ontogenetic indicators in centrosaurine ceratopsids. *Anat Rec (Hoboken)* 292:1485–1500.
- Dal Sasso C, Signore M (1998) Exceptional soft-tissue preservation in a theropod dinosaur from Italy. *Nature* 392:383–387.
- Dal Sasso C, Maganuco S (2011) *Scipionyx samniticus* (Theropoda: Compsognathidae) from the Lower Cretaceous of Italy. *Mem Soc It Sci Nat Museo Civ Stor Nat Milano* 37:1–281.
- Rauhut OWM, Fechner R (2005) Early development of the facial region in a non-avian theropod dinosaur. *Proc Biol Sci* 272:1179–1183.
- Sander PM, Mateus O, Laven T, Knötschke N (2006) Bone histology indicates insular dwarfism in a new Late Jurassic sauropod dinosaur. *Nature* 441:739–741.
- Stein K, et al. (2010) Small body size and extreme cortical bone remodeling indicate phyletic dwarfism in *Magyarosaurus dacus* (Sauropoda: Titanosauria). *Proc Natl Acad Sci USA* 107:9258–9263.
- Smith ND, et al. (2008) A *Megaraptor*-like theropod (Dinosauria: Tetanurae) in Australia: Support for faunal exchange across eastern and western Gondwana in the Mid-Cretaceous. *Proc Biol Sci* 275:2085–2093.
- Choiniere JN, et al. (2010) A basal Alvarezsaurid theropod from the early Late Jurassic of Xinjiang, China. *Science* 327:571–574.
- Benson RBJ, Carrano MT, Brusatte SL (2010) A new clade of archaic large-bodied predatory dinosaurs (Theropoda: Allosauroidea) that survived to the latest Mesozoic. *Naturwissenschaften* 97:71–78.
- Smith ND, Makovicky PJ, Hammer WR, Currie PJ (2007) Osteology of *Cryolophosaurus ellioti* (Dinosauria: Theropoda) from the Early Jurassic of Antarctica and implications for early theropod evolution. *Zool J Linn Soc-Lond* 151:377–421.
- Goloboff PA, Farris JS, Nixon KC (2008) TNT, a free program for phylogenetic analysis. *Cladistics* 24:774–786.
- Rauhut OWM (2003) The interrelationships and evolution of basal theropod dinosaurs. *Spec Pap Palaeont* 69:1–213.
- Göhllich UB, Chiappe LM (2006) A new carnivorous dinosaur from the Late Jurassic Solnhofen archipelago. *Nature* 440:329–332.
- Chiappe LM, Göhllich UB (2010) Anatomy of *Juravenator starki* (Theropoda: Coelurosauria) from the Late Jurassic of Germany. *Neues Jahrbuch für Geologie und Paläontologie, Abhandlungen* 258:257–296.
- Schweigert G (2007) Ammonite biostratigraphy as a tool for dating Upper Jurassic lithographic limestones from South Germany - first results and open questions. *Neues Jahrbuch für Geologie und Paläontologie, Abhandlungen* 245:117–125.
- Mateus O, Walen A, Antunes MT (2006) The large theropod fauna of the Lourinhã Formation (Portugal) and its similarity to the Morrison Formation, with a description of a new species of *Allosaurus*. *New Mexico Mus Nat Hist Sci. Bull* 36:1–7.

29. Soto M, Perea D (2008) A ceratosaurid (Dinosauria, Theropoda) from the Late Jurassic–Early Cretaceous of Uruguay. *J Vert Paleont* 28:439–444.
30. Ostrom JH (1978) The osteology of *Compsognathus longipes* Wagner. *Zitteliana* 4: 73–118.
31. Peyer K (2006) A reconsideration of *Compsognathus* from the Upper Tithonian of Canjuers, southeastern France. *J Vert Paleont* 26:879–896.
32. Rauhut OWM (2003) A tyrannosauroid dinosaur from the Upper Jurassic of Portugal. *Palaentology* 46:903–910.
33. Benson RBJ (2008) New information on *Stokesosaurus*, a tyrannosauroid (Dinosauria: Theropoda) from North America and the United Kingdom. *J Vert Paleont* 28:732–750.
34. Wellnhofer P (2008) *Archaeopteryx. Der Urvogel von Solnhofen* [Archaeopteryx. The primary bird from Solnhofen] (Dr. Friedrich Pfeil, Munich). [in German].
35. Gilmore GW (1920) Osteology of the carnivorous dinosauria in the United States National Museum, with special reference to the genera *Antrodemus* (*Allosaurus*) and *Ceratosaurus*. *B US Nat Mus* 110:1–159.
36. Madsen JH, Welles SP (2000) *Ceratosaurus* (Dinosauria, Theropoda), a revised osteology. *Utah Geol Surv Misc Pub* 00-2:1–80.
37. Galton PM, Jensen JA (1979) A new large theropod dinosaur from the Upper Jurassic of Colorado. *BYU Geol Stud* 26:1–12.
38. Britt BB (1991) Theropods of Dry Mesa Quarry (Morrison Formation, Late Jurassic), Colorado, with emphasis on the osteology of *Torvosaurus tanneri*. *BYU Geol Stud* 37:1–72.
39. Madsen JH (1976) *Allosaurus fragilis*: A revised osteology. *Utah Geol Mineral Surv Bull* 109:3–163.
40. Mateus O (1998) *Lourinhanosaurus antunesi*, a new Upper Jurassic allosauroid (Dinosauria: Theropoda) from Lourinhã, Portugal. *Mem Acad Ciê Lisboa* 37:111–124.
41. Xu X, Guo Y (2009) The origin and early evolution of feathers: Insights from recent paleontological and neontological data. *Vert PalAs* 47:311–329.
42. Ji S, Ji Q, Lü J, Yuan C (2007) A new giant compsognathid dinosaur with long filamentous integuments from Lower Cretaceous of northeastern China. *Acta Geol Sin* 81:8–15.
43. Norell MA, Xu X (2005) Feathered dinosaurs. *Annu Rev Earth Planet Sci* 33:277–299.
44. Mayr G, Peters DS, Plodowski G, Vogel O (2002) Bristle-like integumentary structures at the tail of the horned dinosaur *Psittacosaurus*. *Naturwissenschaften* 89:361–365.
45. Zheng XT, You HL, Xu X, Dong ZM (2009) An Early Cretaceous heterodontosaurid dinosaur with filamentous integumentary structures. *Nature* 458:333–336.
46. Witmer LM (2009) Dinosaur: Fuzzy origins for feathers. *Nature* 458:293–295.
47. Brusatte SL, et al. (2010) The origin and early radiation of dinosaurs. *Earth Sci Rev* 101: 68–100.
48. Bonaparte JF, Novas FE, Coria RA (1990) *Carnotaurus sastrei* Bonaparte, the horned, lightly built carnosaur from the Middle Cretaceous of Patagonia. *Contrib Sci* 416:1–42.
49. Anderson BG, Barrick RE, Droser ML, Stadtman KL (1999) Hadrosaur skin impressions from the Upper Cretaceous Neslen Formation, Book Cliffs, Utah: Morphology and paleoenvironmental context. *Vert Paleont Utah* 99:295–301.
50. Glut DF (2003) *Dinosaurs. The Encyclopedia. Supplement 3* (McFarland & Co, Jefferson, NC).
51. Coria RA, Chiappe LM (2007) Embryonic skin from Late Cretaceous sauropods (Dinosauria) of Auca Mahuevo, Patagonia, Argentina. *J Paleontol* 81:1528–1532.
52. Xing L, Peng G, Shu C (2008) Stegosaurian skin impressions from the Upper Jurassic Shangshaximiao Formation, Zigong, Sichuan, China: A new observation. *Geol Bull China* 27:1049–1053.
53. Bell PR (2012) Standardized terminology and potential taxonomic utility for hadrosaurid skin impressions: A case study for *Saurolophus* from Canada and Mongolia. *PLoS ONE* 7:e31295.
54. Crowe R, Niswander L (1998) Disruption of scale development by Delta-1 misexpression. *Dev Biol* 195:70–74.
55. Widelitz RB, Jiang TX, Lu J, Chuong CM (2000)  $\beta$ -catenin in epithelial morphogenesis: Conversion of part of avian foot scales into feather buds with a mutated  $\beta$ -catenin. *Dev Biol* 219:98–114.
56. Harris MP, Fallon JF, Prum RO (2002) Shh-Bmp2 signaling module and the evolutionary origin and diversification of feathers. *J Exp Zool* 294:160–176.
57. Dhauailly D (2009) A new scenario for the evolutionary origin of hair, feather, and avian scales. *J Anat* 214:587–606.
58. Xu X, et al. (2012) A gigantic feathered dinosaur from the lower cretaceous of China. *Nature* 484:92–95.
59. Bakhurina NN, Unwin DM (1995) in *Sixth Symposium on Mesozoic Terrestrial Ecosystems and Biota*, eds Sun A, Wang Y (China Ocean, Beijing), pp 79–82.
60. Wang X, Zhou Z, Zhang F, Xu X (2002) A nearly completely articulated rhamphorhynchoid pterosaur with exceptionally well-preserved wing membranes and “hair” from Inner Mongolia, northeast China. *Chin Sci Bull* 47:226–230.
61. Zhou Z (2004) The origin and early evolution of birds: Discoveries, disputes, and perspectives from fossil evidence. *Naturwissenschaften* 91:455–471.
62. Sawyer RH, Knapp LW (2003) Avian skin development and the evolutionary origin of feathers. *J Exp Zool B Mol Dev Evol* 298:57–72.
63. Alibardi L, Sawyer RH (2006) Cell structure of developing downfeathers in the zebra finch with emphasis on barb ridge morphogenesis. *J Anat* 208:621–642.
64. Alibardi L, Toni M (2008) Cytochemical and molecular characteristics of the process of cornification during feather morphogenesis. *Prog Histochem Cytochem* 43:1–69.
65. Prum RO (1999) Development and evolutionary origin of feathers. *J Exp Zool* 285: 291–306.
66. Prum RO, Brush AH (2002) The evolutionary origin and diversification of feathers. *Q Rev Biol* 77:261–295.

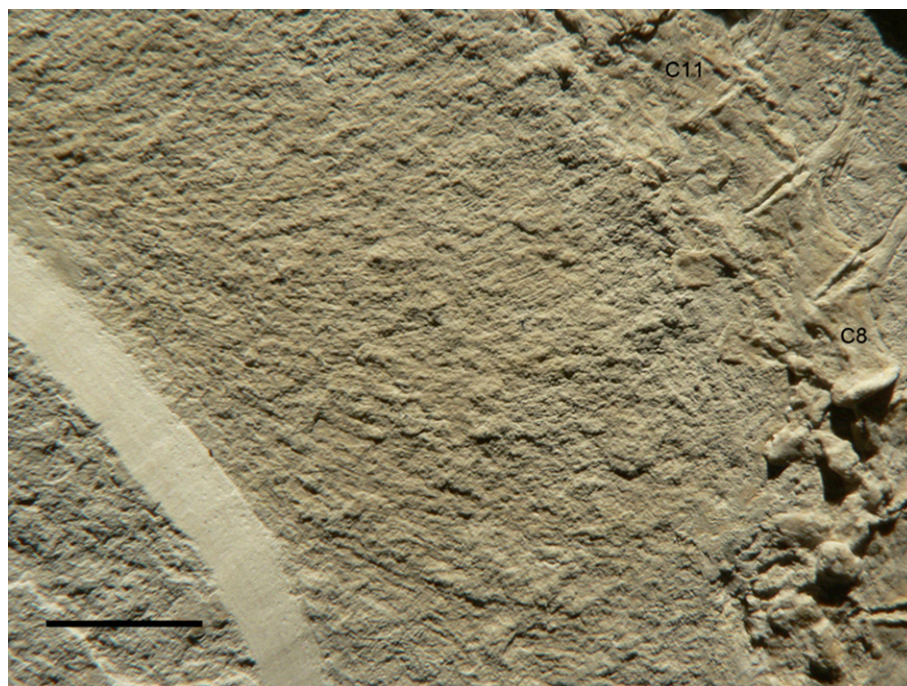


Fig. 51. Impressions of filaments dorsal to anterior caudal vertebrae under normal light. C, caudal vertebra. (Scale bar: 10 mm.)

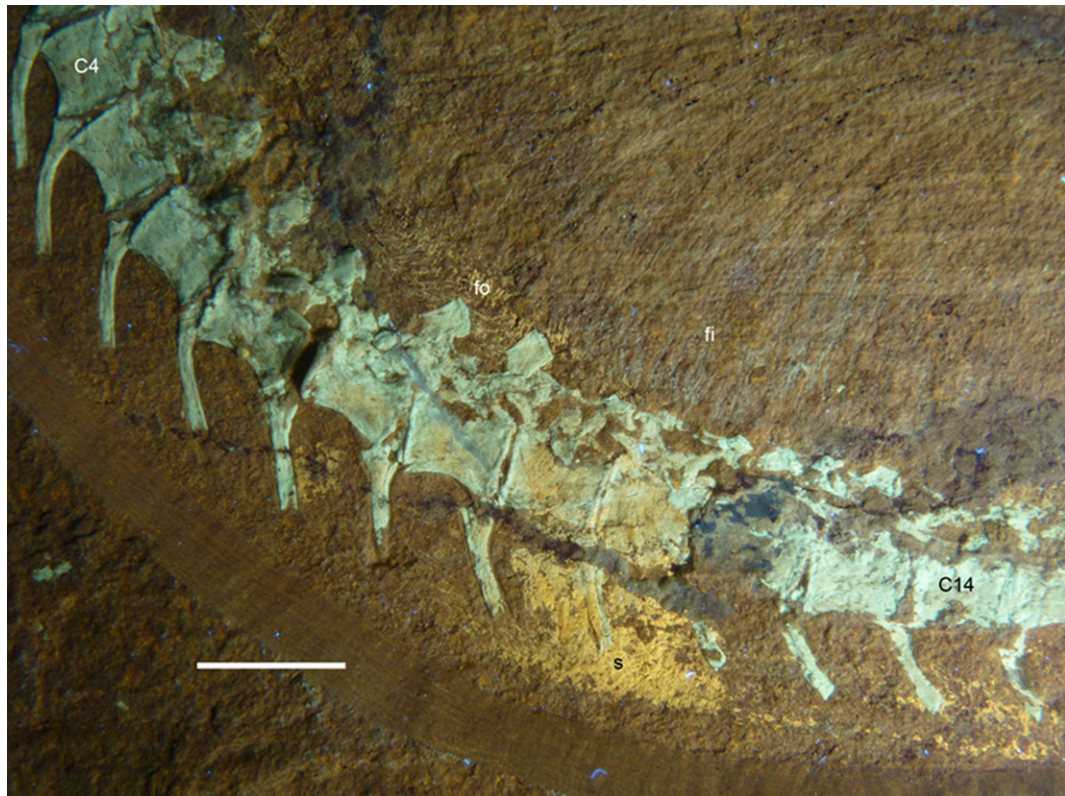


Fig. 52. Soft tissue preservation in the anterior caudal region of *Sciurumimus* under UV light. C, caudal vertebra; fi, filaments; fo, possible follicles at the base of filaments; s, skin. (Scale bar: 10 mm.)

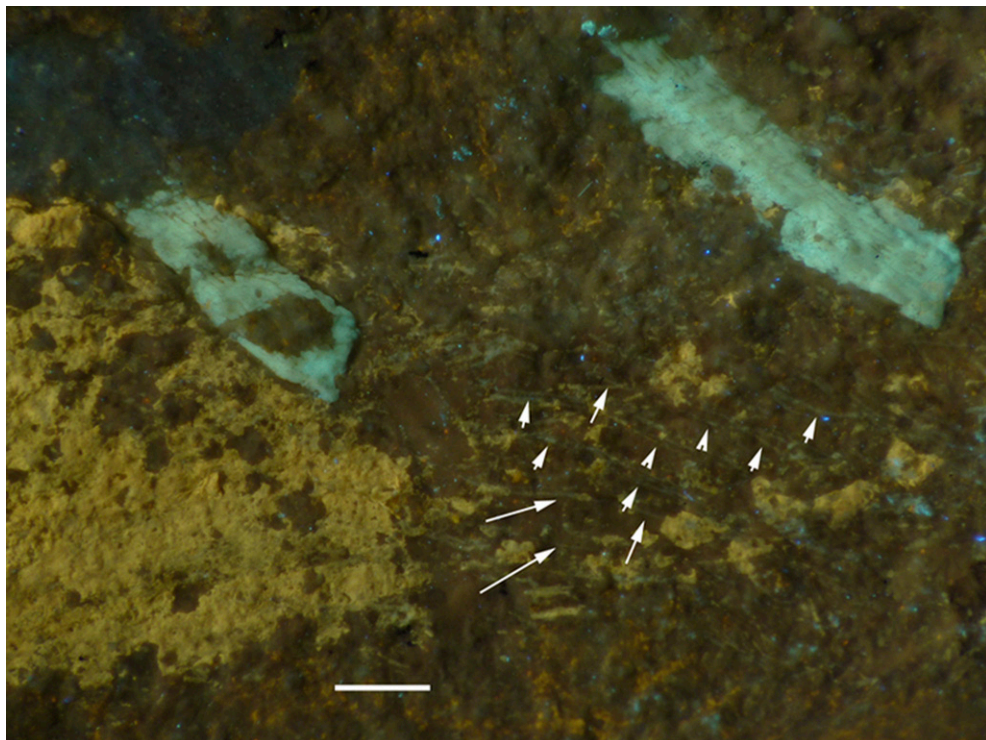
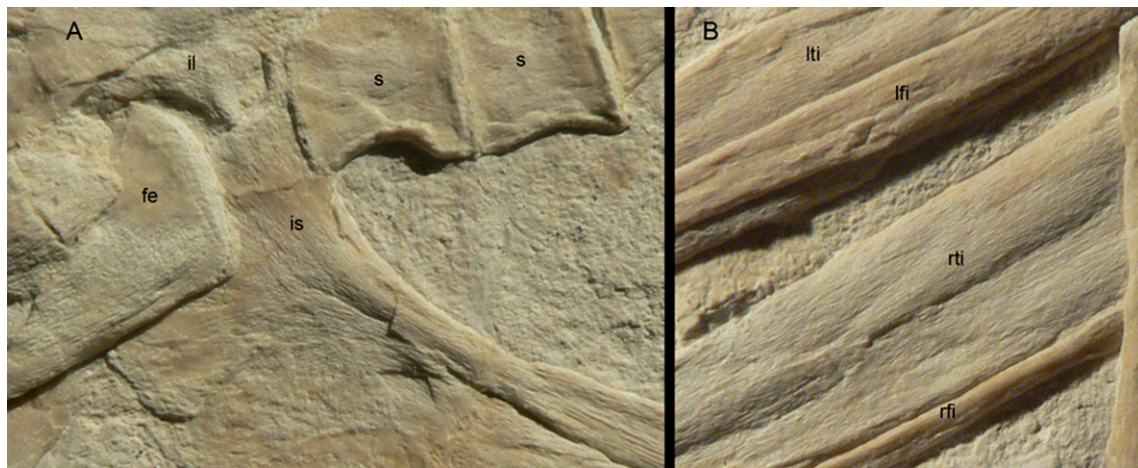


Fig. 53. Short filaments on the ventral tail flank below the 12th and 13th caudal vertebra. Arrows and arrowheads point to single filaments.



**Fig. S4.** Lateral side of the left dentary of *Sciurumimus* showing striated texture of bone surface.



**Fig. S5.** Striated texture of bone surface in sacral vertebrae and pelvic and limb elements of *Sciurumimus*. (A) Ischial peduncle of the left ilium, posterior sacral vertebrae, and proximal end of femur and ischium. (B) Tibiae and fibulae. fe, femur; il, ilium; is, ischium; lfi, left fibula; lti, left tibia; rfi, right fibula; rti, right tibia; s, sacral vertebra.



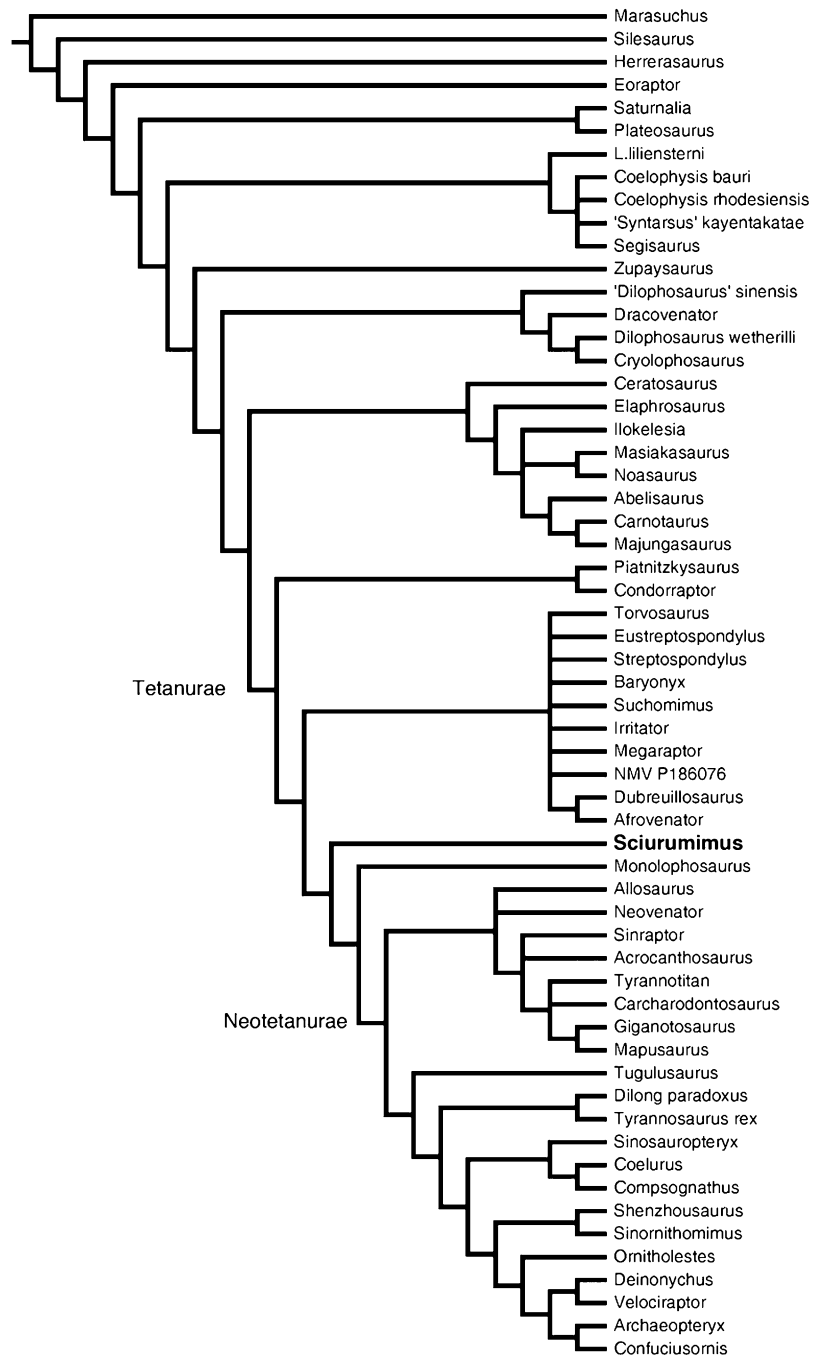


Fig. S6. Strict consensus cladogram of the analysis based on Smith et al. (19).



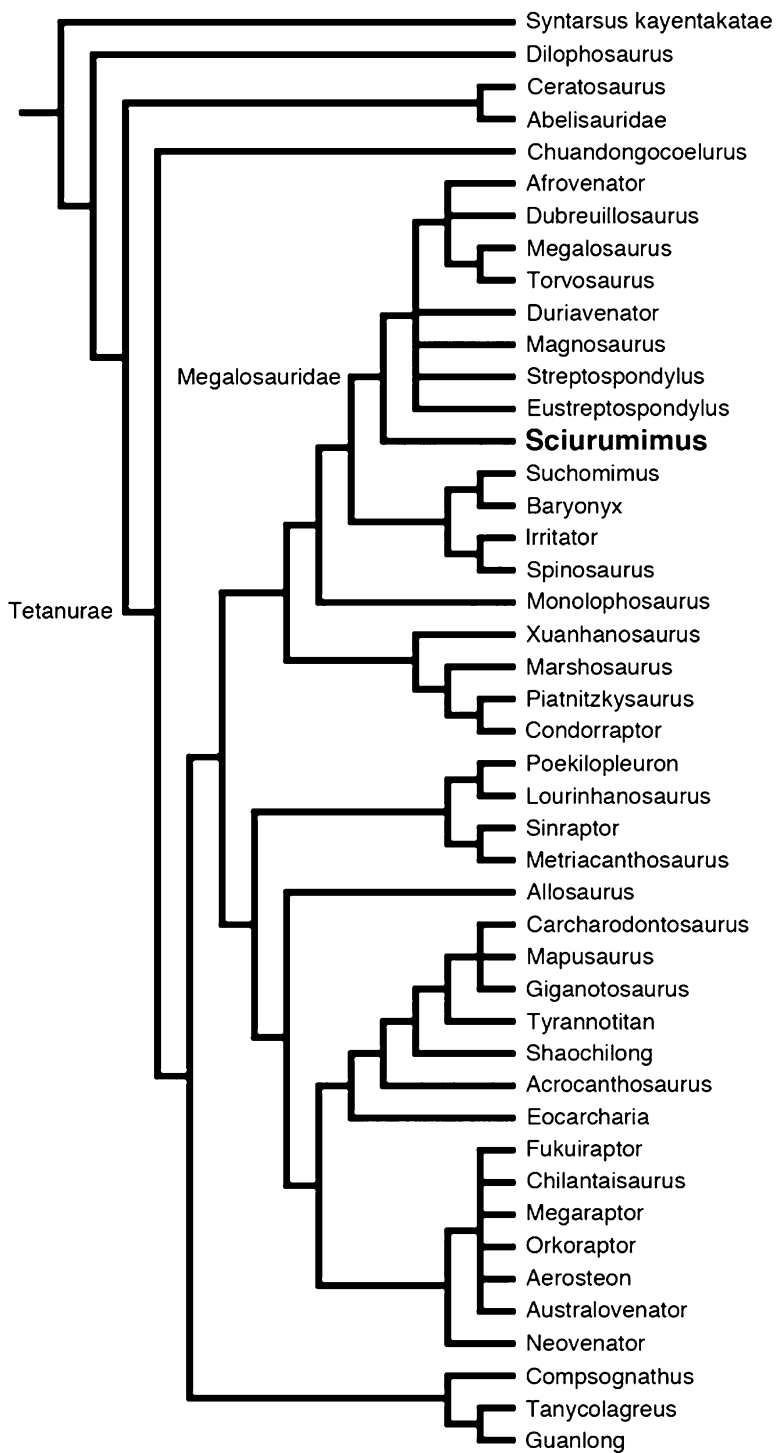


Fig. 58. Reduced consensus tree of the analysis based on the matrix of Benson et al. (21).

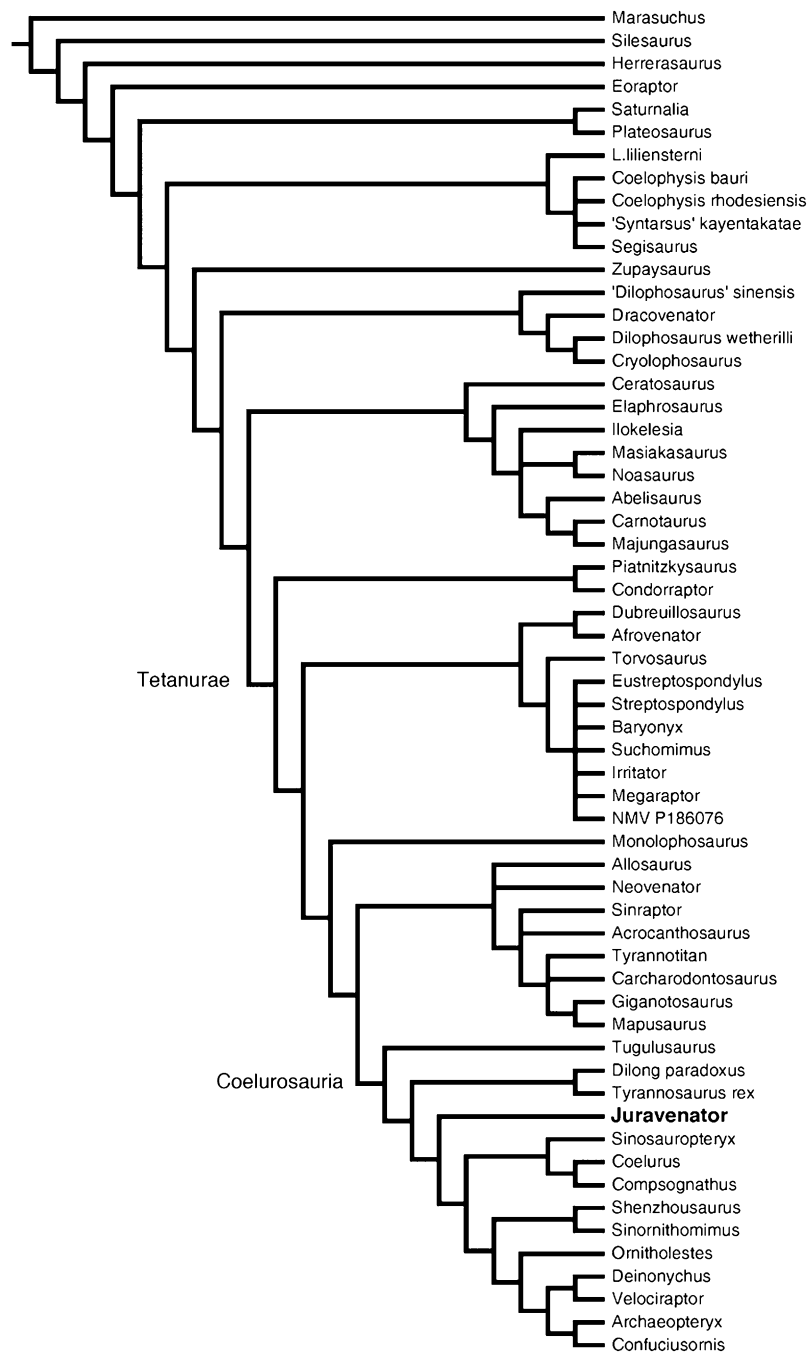
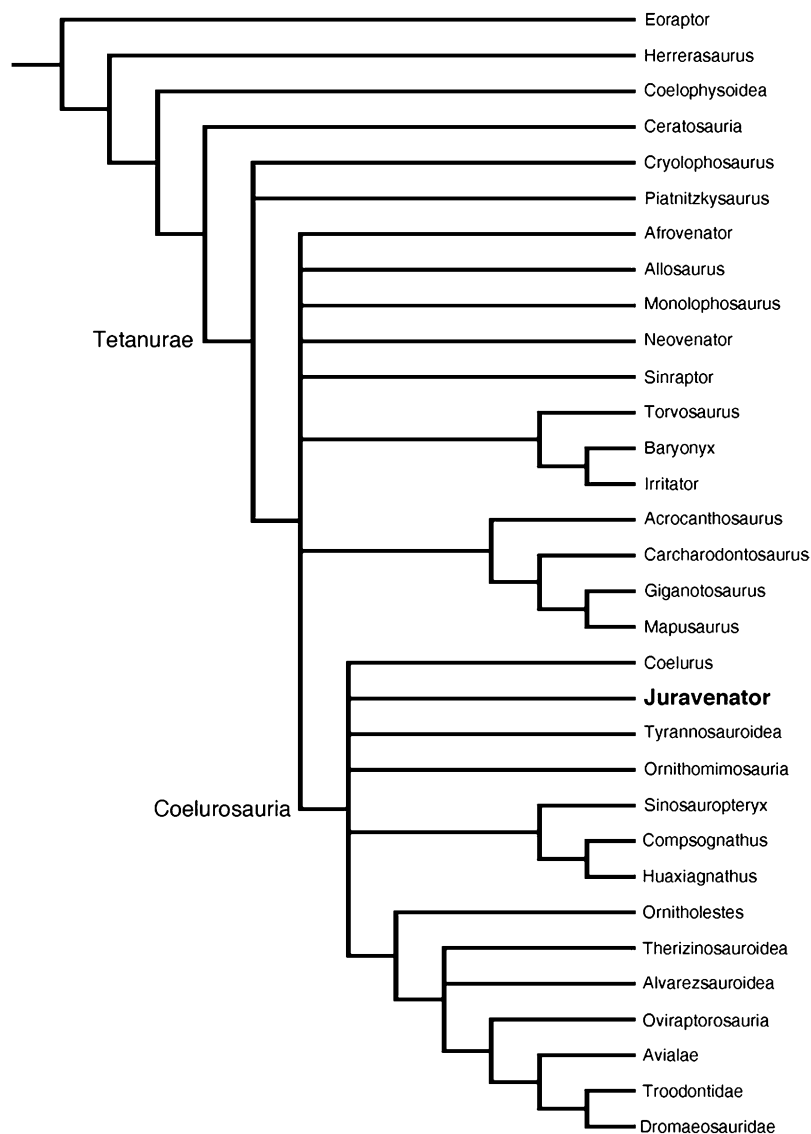


Fig. S9. Phylogenetic analysis of *Juravenator*, excluding *Sciurumimus* based on the matrix of Smith et al. (19).



**Fig. S10.** Phylogenetic analysis of *Juravenator*, excluding *Sciumimus*, based on the matrix of Choiniere et al. (20). Several clades have been collapsed for clarity.

**Table S1.** Comparison of selected measurements of *Juravenator* and *Sciumimus*

Measurement	<i>Juravenator</i> (in mm)	<i>Sciumimus</i> (in mm)
Skull length	82	79
Scapula length	42	42
Humerus length	27	26.8
Radius length	ca. 19	17
Mc II length	9	8.8
Femur length	52	50.6
Tibiotarsus length	58.1	54.2
Mt III length	34	32.1

Measurements of *Juravenator* are from ref. 26.